Published in final edited form as:
Cancer Res. 2012 February 15; 72(4): . doi:10.1158/0008-5472.CAN-11-0210.

Dysregulation of Ezrin phosphorylation prevents metastasis and alters cellular metabolism in osteosarcoma

Ling Ren[1], **Sung-Hyeok Hong**[1], **Qing-Rong Chen**[2], **Joseph Briggs**[1], **Jessica Cassavaugh**[1], **Satish Srinivasan**[3], **Michael M. Lizardo**[1], **Arnulfo Mendoza**[1], **Ashley Y. Xia**[4], **Narayan Avadhani**[3], **Javed Khan**[2], and **Chand Khanna**[1]

[1]Tumor and Metastasis Biology Section, Center for Cancer Research, National Cancer Institute

[2]Oncogenomics Section, Pediatric Oncology Branch, Center for Cancer Research, National Cancer Institute

[3]Department of Animal Biology, School of Veterinary Medicine, University of Pennsylvania

[4]Office of Biomedical Informatics, Division of Allergy, Immunology and Transplantation, National Institute of Allergy and Infectious Diseases

Abstract

Ezrin links the plasma membrane to the actin cytoskeleton where it plays a pivotal role in the metastatic progression of several human cancers (1, 2), however, the precise mechanistic basis for its role remains unknown. Here we define transitions between active (phosphorylated open) and inactive (dephosphorylated closed) forms of Ezrin that occur during metastatic progression in osteosarcoma. In our evaluation of these conformations we expressed C-terminal mutant forms of Ezrin that are open (phosphomimetic T567D) or closed (phosphodeficient T567A) and compared their biological characteristics to full length wild-type Ezrin in osteosarcoma cells. Unexpectedly, cells expressing open, active Ezrin could form neither primary orthotopic tumors nor lung metastases. In contrast, cells expressing closed, inactive Ezrin were also deficient in metastasis but were unaffected in their capacity for primary tumor growth. By imaging single metastatic cells in the lung, we found that cells expressing either open or closed Ezrin displayed increased levels of apoptosis early after their arrival in the lung. Gene expression analysis suggested dysregulation of genes that are functionally linked to carbohydrate and amino acid metabolism. In particular, cells expressing closed, inactive Ezrin exhibited reduced lactate production and basal or ATP-dependent oxygen consumption. Collectively, our results suggest that dynamic regulation of Ezrin phosphorylation at amino acid T567 that controls structural transitions of this protein plays a pivotal role in tumor progression and metastasis, possibly in part by altering cellular metabolism.

Keywords

Ezrin; ERM; tumor metastasis

Introduction

Ezrin, a cell membrane to cytoskeleton linker protein, plays an important role in the metastatic progression of several tumors (1–5). However, the mechanisms by which Ezrin contributes to the metastatic phenotype of cancer are largely unknown. Ezrin is a member of the ERM (Ezrin-Radixin-Moesin) protein family, which provides a physical link from F-Actin to cell membrane-associated proteins (6, 7). This linker function makes ERM proteins essential for fundamental cellular processes, including the determination of cell shape, polarity and formation of surface structures, cell adhesion, motility, cytokinesis, phagocytosis and integration of membrane transport with signaling pathways (8–10).

Phosphorylation and dephosphorylation of Ezrin at T567 has been identified as a critical step in the conformational activation and deactivation of Ezrin (11, 12). Ezrin is proposed to exist in a dormant form in which the C-terminal tail binds to and masks the N-terminal FERM domain. In our previous studies of Ezrin and tumor metastasis, we were surprised to find that Ezrin was not constitutively phosphorylated but rather was dynamically regulated during metastatic progression (13). Metastatic OS cells expressed phosphorylated ERM early after their arrival in the lung. There was then a loss of phosphorylated ERM within the growing metastatic lesion, followed by a re-expression of phosphorylated ERM only at the invasive front of larger metastatic lesions (13). The activation of Ezrin is mediated by both exposure to PIP2 and phosphorylation of the C-terminal threonine (T567) (11). The deactivation of Ezrin is also important for physiologic functions including the dynamics of Actin-rich membrane projections. ERM dephosphorylation (Moesin T558) may be a crucial step for lymphocyte adhesion and transendothelial migration. The disassembly of microvilli on lymphocyte cell surfaces caused by dephosphorylation of Moesin facilitates the cell-cell (lymphocyte-endothelium) contact (9).

Given the apparent dynamic regulation of Ezrin in open and closed conformations, we now evaluate their relative contributions, during progression of OS, by expressing Ezrin mutants that are either constitutively activated/open (EzrinT567D) or constitutively closed (T567A) in cells. Surprisingly, OS cells expressing constitutively open Ezrin (T567D) could neither form primary orthotopic tumors, nor grow lung metastases. Over-expression of EzrinT567A, significantly diminished both experimental and spontaneous metastasis, but did not affect the orthotopic primary tumor development. The behavior of the T567A expressing cells is similar to approximately 30% of OS patients. In these patients primary tumor development occurs but metastasis to distant sites does not occur (14). This is in distinction to the majority of patients who progress to develop metastatic disease following management of the primary tumor alone. At this time there are no means to identify those patients at high or low risk for metastasis or understand the biological determinants of these phenotypes. Using Single Cell VideoMicroscopy (SCVM) techniques (15), we have defined a biological mechanism to explain the effects of Ezrin dysregulation on metastasis. Indeed, cells over-expressing EzrinT567A undergo increased apoptotic death early after their arrival in the lung. To begin to understand this mechanism, gene expression analysis of OS cells over-expressing EzrinT567A found a significant over-expression of genes whose functions were consistently connected to cellular metabolism. Functional validation of these gene expression data confirmed alterations in basal cellular metabolism and mitochondrial function in the less metastatic EzrinT567A mutant cells and in unrelated pairs of high and low metastatic OS cells that differentially express Ezrin. Collectively, these data suggest that both open and closed conformations of Ezrin contribute to the metastatic phenotype of OS cells. In a constitutively closed conformation the ability of these cells to overcome apoptosis early after the arrival of cells in the lung was impaired resulting in the inhibition of metastasis. Finally, Ezrin dysregulation was uniquely associated with alterations in cellular metabolism. Future studies will characterize these alterations in cellular metabolism and the association with the biology of metastasis.

Materials and methods

Cells, Transfection and Cellular assays

Murine (K7M2 and K12) (16) and human MG63 (ATCC, Mabassas, VA), MG63.2 (kindly provided from Dr. Hue Luu) (17) OS cells were grown in DMEM (Invitrogen, Calsbad, CA) containing 10% fetal bovine serum, at 37°C in 5% CO_2. Geneticin (G418; 0.8 mg/ml) (Invitrogen) was added to the medium of cells transfected with Ezrin mutant constructs derived as described in the Supplementary Methods. These cells were used in assays of cell

proliferation, migration, invasion, and anchorage independent growth are described in the Supplementary Methods, as previously reported (13).

Confocal microscopy

GFP expressing Ezrin mutant cells were grown in chamber slides. After fixing cells with 3.7 % formaldehyde, chambers were removed and slides were cover slipped. Digital images were acquired with a Zeiss LSM 510 confocal system using a 63× 1.4NA Plan-Apochromat oil immersion objective.

Western blot analysis and Triton X-100 fractionation

Total protein extracts were separated by 4–12% or 4–20% SDS-PAGE electrophoresis, transblotted onto a nitrocellulose membrane and incubated with the following antibodies: anti-GFP 1:2500 (Chemicon, Temecula, CA), anti-Ezrin 1:4000 (Sigma, Carlsbad, CA), anti-phospho-Ezrin(T567)/Radixin(T564)/Moesin(T558) 1:1000 (Cell Signaling, Danvers, MA), anti-Merlin 1:3000 (kindly provided by Dr. Anthony Bretcher), anti-Radixin 1:20,000 (Abcam, Cambridge, MA), anti-Moesin (Cell Signaling Danvers, MA) and anti-β-Actin 1:10,000 (Sigma, Carlsbad, CA). Detergent-soluble (Actin-free) and insoluble (Actin-enriched) fractions of cellular proteins were derived by Triton X-100 fractionation (See Supplementary Methods).

Experimental metastasis and spontaneous metastasis

As previously described (18), tail vein injection of K7M2 or MG63.2 cells, included 10^6 or 10^4 cells respectively (minimum of 10 mice/group. For spontaneous metastasis, orthotopic transplantation of 2×10^6 viable cells to the para-osseous proximal tibia was as previously described (18) using a minimum of 15 mice/group. The volume of orthotopic tumor was calculated as previously reported (19). Tumor bearing limbs were resected at a tumor size of 1.5–2.0 cm^3. Mice were then evaluated every other day for the development of metastasis-associated morbidity. Complete necropsy validated the presence of pulmonary metastases in all mice. All animal studies were done with the approval of the Animal Care and Use Committee of the National Cancer Institute.

Single Cell VideoMicroscopy (SCVM) and Pulmonary Metastasis Assay (PuMA)

Detection of apoptosis in single tumor cells within the lung was accomplished using a modification of SCVM assay (1, 15) that detected Caspase activation in single tumor cells by SR-FLIVO (Immunochemistry Technologies, LLC, Bloomington, MN). Human (MG63.2) and murine (K7M2) OS cells expressing GFP tagged EzrinT567A mutant and GFP alone (5×10^5) were injected through tail vein into mice (n=3–5/group) as previously described for SCVM. SR-FLIVO reagent was IV injected 2 h later and allowed to circulate for 60 min. The lungs were excised, washed in PBS and imaged en bloc using LEICA-DM IRB inverted fluorescence microscope (above) at defined time points. Image analysis included both green (GFP-expressing) tumor cells and red (SR-FLIVO-staining) apoptotic cells. The colocalization of red SR-FLIVO staining within GFP-expressing tumor cells was then confirmed by performing confocal microscopy on 15 μm frozen sections stained with 4', 6-diamidino-2-phenylindole (DAPI) in PBS (1 μg/ml) for 5 minutes, rinsed in PBS and mounted in Vectashield (Burlingame, CA). Experiments were repeated 3 times. The *ex vivo* evaluation of Ezrin mutant and control expressing cells in whole lung cultures was performed using the Pulmonary Metastasis Assay (PuMA) as previously described and summarized in the Supplementary Methods (20).

DNA array and Gene Set Enrichment Analysis

RNA samples from K7M2/GFP, K7M2/EzrinT567A-GFP were prepared using Qiagen RNA mini kit (Qiagen, Hilden, Germany) according to manufacturer's directions. RNA quality was assessed using an Agilent 2100 Bioanalyzer. All samples were prepared for cRNA hybridization via the Affymetrix One-cycle Eukaryotic Target Labeling Assay according to manufacturer's instructions. Once the cRNA was cleaned and fragmented, it was individually hybridized to Affymetrix Mouse Genome 430 2.0 arrays. All samples were prepared and hybridized at the National Cancer Institute (NCI) DNA array core facility. The .CEL files were exported from Affymetrix AGCC software and normalized with RMA-sketch from Affymetrix Power Tools. The .CEL files and the processed data have been uploaded to NCBI Gene Expression Omnibus (GEO accession: GSE33897). To investigate the pathways and gene sets that were differentially regulated in T567A mutants compared to GFP controls, Gene Set Enrichment Analysis (GSEA) method (21) was applied to the global gene expression profiles with a weighted enrichment statistic corresponding to a weighted Kolmogorov-Smirnov-like statistics, and genes were ranked using $\log_2$ ratio of gene expression in T567A mutants versus GFP control (22) (Supplementary Methods).

Measurements of extracellular acidification and oxygen consumption rate

The XF24 Extracellular Flux Analyzer (Seahorse Bioscience, North Billerica, MA) was used to detect rapid, real time changes in cellular respiration and glycolysis rate. Analysis of extracellular acidification rate (ECAR) reflects lactate excretion and serves as an indirect measure of glycolysis rate, while oxygen consumption rate (OCR) reflects cellular respiration and is directly determined (23). K7M2 and MG63.2 cells expressing EzrinT567A–GFP or GFP alone were tested along with 2 other pairs of osteosarcoma cells (MG63.2/MG63 and K7M2/K12) in which high and low Ezrin expression was associated with high and low metastatic phenotypes, respectively. The cells were seeded in XF24 microplates (25,000 cells/well) the day before the measurements. All measurements were performed following manufacturer's instructions, and the observed rates are reported in pMoles/min for OCR and mpH/min for ECAR. The experiment was repeated 3 times.

Results

Expression of Ezrin mutants alters the phenotype of OS cells

The highly metastatic murine K7M2 OS cells (wild-type, WT) were transfected with a pEGFP-N1 plasmid alone (GFP) or as a GFP fusion protein with Ezrin (Ezrin-GFP), or the Ezrin mutants (EzrinT567A-GFP, or EzrinT567D-GFP). Multiple single stable clones were established by G418 selection. Western blot analysis confirmed the expression of Ezrin and Ezrin mutants (Fig. 1A). The localization of Ezrin mutants was observed by confocal fluorescent microscopy (Fig. 1B). As expected, GFP alone was expressed in the entire cell (both nucleus and cytosol). Ezrin-GFP and EzrinT567A-GFP were expressed in the cytoplasm with limited expression on the cell membrane. Consistent with our expectations of the active (open) Ezrin conformation, EzrinT567D-GFP localized almost exclusively at the cell membrane and at cell surface structures. Over-expression of EzrinT567D mutant resulted in changes in cell morphology (Fig. S1A). The subcellular location of Ezrin mutants was assessed using a Triton X-100 fractionation followed by Ezrin immunoblotting (Fig. 1C). The majority of endogenous Ezrin from all samples was distributed in the Triton-X 100 soluble portion; pERMs were mainly in the insoluble fractions (data not shown). This was also true for the exogenously expressed wild type Ezrin-GFP and EzrinT567A-GFP. In contrast, EzrinT567D-GFP proteins were mainly localized in the insoluble fraction. No significant change in the expression of other members of ERM family proteins (Radixin, Moesin, and Merlin) was seen following EzrinT567 mutant over-expression (Fig. S1B).

EzrinT567D mutants have multiple defects in the metastatic phenotype

The proliferation rates of Ezrin mutant expressing cells were not distinct from control cells using the CCK-8 cell proliferation assay (Fig. 2A) or by counting of Trypan Blue excluded cells (not shown). These data were verified in human OS cells (MG63.2) (data not shown). Over-expression of EzrinT567D-GFP resulted in several defects in the metastatic phenotype. As shown in figure 2B, EzrinT567D-GFP mutant cells had reduced migration ($p<0.0001$) and invasion ($p<0.0001$) compared to GFP expressing cells. Furthermore, EzrinT567D-GFP expressing cells lost their ability for anchorage-independent growth on agarose ($p<0.0001$), Matrigel and collagen I matrices (Fig. 2C & 2D) and had limited heterotypic adhesion to laminin. No inhibition of heterotypic adhesion was seen for other extra-cellular matrices (fibronectin, poly-o-D-lysine, collagen I, and collagen IV; data not shown). *In vitro* functional consequences of EzrinT567A-GFP expression were subtle and included a reduction in soft agar colony size ($p<0.005$), but no change in colony numbers (Fig. 2C & 2D) and a modest inhibition of cell migration.

Over-expressing EzrinT567D mutants completely suppresses primary tumorgenicity

To evaluate contributions of the Ezrin mutants on OS biology and progression *in vivo*, we injected GFP, Ezrin-GFP, EzrinT567D-GFP and EzrinT567A-GFP expressing cells to appendicular orthotopic sites in mice. GFP and EzrinT567A-GFP injected animals formed tumors that were readily detectable at two weeks. Primary tumor growth rates (Fig. 3A) and histological features (cellular morphology and architecture, necrosis, stromal component, vascularity, and mitotic index) were similar between EzrinT567A-GFP expressing cells and cells expressing GFP alone. Surprisingly, no tumors were detected over 200 days following injection of EzrinT567D-GFP expressing cells (Fig. 3A). Microscopic examination of the orthotopic sites of injection confirmed clearance of all EzrinT567D-GFP cells within 7 days, with evidence of Caspase 3 cleavage in tumor cells as early as 2 days (Fig. S2B).

Over-expressing EzrinT567A mutants specifically suppresses tumor metastasis

Following primary tumor growth and resection of tumor-bearing limbs, mice receiving EzrinT567A and control tumors were followed for development of spontaneous metastasis. Over 50% mice receiving OS cells expressing GFP vector alone (Fig. 3B) were sacrificed as a result of lung metastases between 50 and 140 days of tumor-bearing limb resection. By comparison, no mice bearing EzrinT567A-GFP developed lung metastasis (necropsy and histologically microscopic confirmed). To further confirm the inhibition of metastasis following over-expression of EzrinT567A mutants, experimental metastasis assays were performed with control and mutant expressing cells. Cells expressing wild type Ezrin-GFP were included in this experiment to verify that phenotypes observed with Ezrin mutants was not caused by Ezrin over-expression alone. As expected, mice injected with GFP and Ezrin-GFP expressing cells were euthanized due to lung metastases (100%, 10/10 mice; Fig. 3C). Mice receiving cells expressing EzrinT567A-GFP or EzrinT567D–GFP mutants had no metastasis at the termination of the experiment (day 90) (Fig. 3C and Fig. S2C). Similar results were seen with cells from 2 additional clones of each mutant (data not shown). Necropsy and examination of serial histological sections showed occasional micro-metastases in EzrinT567A-GFP bearing mice. This metastasis specific defective phenotype associated with EzrinT567A-GFP expression was also observed in a second highly metastatic human OS cell line model (MG63.2; Fig. S2E). To rule out the possibility that EzrinT567D–GFP expressing cells were inducing a GFP targeted immune rejection, experimental metastasis experiments were repeated in immuno-deficient SCID mice. Again, mice with GFP expressing cells were euthanized due to pulmonary metastasis (100%, 10/10 mice), while mice receiving EzrinT567D–GFP expressing cells did not develop metastasis at the termination of the experiment (100 day; Fig. S2D). A summary of *in vitro* and *in vivo*

phenotypes of osteosarcoma cells over-expressing Ezrin mutants at T567 is shown in table 1.

Cells expressing EzrinT567A mutants do not progress following their arrival in the lung and undergo increased apoptotic death

The phenotype of EzrinT567A expressing cells in mice was similar to clinical observations in approximately 20% of human OS patients who do not develop metastasis to distant sites (14). This similarity coupled with the fact that these patients are not currently distinguishable at presentation led us to further explore the biology of the EzrinT567A mutants. Using an *ex vivo* pulmonary metastasis assay (PuMA) and single cell videomicroscopy (SCVM) (1, 15, 20), we identified a biological mechanism to explain the failure of metastasis. Dysregulation of Ezrin yielded its impact on early events following the arrival of metastatic cells in the lung (Fig. 3D). Within the *ex vivo* PuMA, metastatic cancer cells progress from single discrete cells to multicellular metastatic cellular clusters over 7 days. EzrinT567A-GFP cells failed to progress beyond single cells. Indeed, these cells progressively declined in number between days 4 and 7 *ex vivo*. Using epifluorescence widefield SCVM, the immediate impact of Ezrin dysregulation on early metastastic progression and metastatic inefficiency was confirmed (Fig. 4A). As previously reported most metastatic tumor cells that arrive in the lung are not retained, do not form metastases due to metastatic inefficiency (24–27). Within 6 hours of their arrival in the lung, approximately 50% of both wild-type and GFP expressing cells were not evident in the lung compared to over 80% of EzrinT567A-GFP cells. To elucidate a biological mechanism explaining the defect in metastatic phenotype, a modification of the SCVM imaging technique was performed to allow the fluorescent visualization of Caspase activation in single cells, early after their arrival in the lung (Fig. 4B). The expression of EzrinT567A-GFP was associated with a significant increase in single cell apoptosis (measured by Caspase activation) within 2 h of tumor cell arrival in the lung in both murine (K7M2) and human OS cells (MG63.2; Fig. 4B).

Gene expression studies of EzrinT567A mutants suggests alterations in cellular metabolism

To begin to understand the impact of EzrinT567A expression on the metastatic phenotype and more specifically the survival of tumor cells at secondary sites, microarray comparisons were undertaken to define differences in gene expression between EzrinT567A-GFP and GFP alone expressing cells. Functional assessment using Gene Set Enrichment Analysis (GSEA) of differentially expressed genes was conducted. A robust list of significant gene functions collectively linked to altered cellular metabolism was seen in association with EzrinT567A-GFP expression (Fig. 5A&B, Table 2). Gene functions that were suppressed following EzrinT567A-GFP expression were linked to cell cycle functions. The significance of these changes in cell cycle functions is unclear given that no changes in cell proliferation or primary tumor growth *in vivo* were noted between cells expressing EzrinT567A-GFP and controls (Fig. 2A and Fig. 3A).

EzrinT567A mutants have altered cellular metabolism

To functionally validate gene expression and Gene Set Enrichment Analysis (GSEA) we asked if baseline changes in cellular metabolism occurred following expression of EzrinT567A-GFP in cells. Using extracellular flux analysis (EFA), markers of cellular respiration and glycolysis rate were assessed from cells *in vitro*. Suppression of oxygen consumption (OCR) and glycolysis (ECAR) were found in cells expressing EzrinT567A-GFP compared to control cells (Fig. 5C). Confirmation of these results was provided through the study of distinct high and low metastatic OS cells in which Ezrin was

differentially expressed (in clonal pairs; MG63.2/MG63; K7M2/K12) (Fig. 5C) (17, 18). Consistent trends taken from these studies indicated that low metastatic, low Ezrin expressing cells simultaneously had reduced basal OCR and ECAR compared to high metastatic, high Ezrin expressing cells. The proportion of oxygen consumed in these cells coupled to ATP synthesis was determined by treatment of cells with oligomycin, an inhibitor of ATP synthase. As shown in Supplementary Figure 3, a significantly higher percentage of oxygen consumed by cells expressing high Ezrin was coupled to ATP synthesis compared to cells expressing low Ezrin. Total cellular ATP levels were measured in clonal pairs of cells expressing either EzrinT567A or in cells with high and low levels of Ezrin. Although, modest, Ezrin dysregulation or suppression was associated with lower total ATP levels than corresponding clonal pairs expressing more wild-type or high Ezrin (data not shown). This is in accordance with higher ATP coupled respiration in more metastatic, Ezrin expressing cells than less metastatic cells. Consistent with these data, highly metastatic cells that express wild-type or high Ezrin had greater respiratory capacity than cells with dysregulated or low levels of Ezrin expression (Fig. S3). Respiratory capacity was assessed by treatment with an uncoupler of respiration (FCCP), followed by measurement of OCR. Based on these data we hypothesize that Ezrin dysregulation leads to impaired metabolic and respiratory competency in cells.

Discussion

Ezrin has been shown to be expressed in most human cancers and is linked to progression in several cancers including pediatric sarcoma, carcinoma of endometrium, breast, colon, ovary, in uveal and cutaneous melanoma, brain tumors, and most recently soft tissue sarcoma (1, 2, 5, 28–30). Phosphorylation of Ezrin at T567 is believed to be a necessary step in the activation of Ezrin (11, 31). Contrary to our expectation, the so-called “active” phoshorylated form of Ezrin was not constitutively expressed during metastasis. Rather, phosphorylation of Ezrin at T567 was dynamically regulated during metastatic progression (13). Present studies were undertaken in order to understand what roles the phosphorylated and dephosphorylated forms of Ezrin have on OS progression and to determine how these findings may more broadly integrate into our understanding of cancer metastasis.

Several models describing the process of metastatic progression from a primary tumor to distant metastatic sites have been established (32–35). Several genes and the regulation of several others contribute to discrete steps in the metastatic cascade and collectively confer the metastatic phenotype on a cancer. Interestingly, based on work presented herein, the ability of Ezrin to contribute to tumor cell survival during the early stages of lung colonization appears to be in part the result of transitions between open and closed conformations of Ezrin. Indeed, the overexpression of Ezrin mutants that are fixed in either open (T567D) or closed (T567A) conformations blocks both tumor development and metastasis or metastasis alone, respectively. These data support the contention that distinct and necessary roles exist for both conformations of Ezrin during tumor progression in OS (36–39). The fact that over-expression of the activated form of Ezrin (EzrinT567D–GFP) completely blocked both primary tumor growth and metastasis was surprising. Over-expression of either Ezrin mutant did not influence cell proliferation *in vitro*. However, the expression of EzrinT567D–GFP led to several changes in cellular phenotype that predicted impaired tumor progression and metastasis. This included impaired cell migration, invasion, adhesion, and growth in soft agar. Previous studies of T567 mutation in Ezrin, Radixin T564 and Moesin T558 have produced striking morphological anomalies in a variety of cell systems. COS7 cells and LLC-PK1 cells display extensive formation of microvillar structures when expressing active ERM mutants (31, 40). We observed similar morphological changes in cells following the expression of EzrinT567D–GFP in OS cells (Fig. S1B) and observed the localization of EzrinT567D–GFP at the cell cortex. The

formation of these structures generally results in reduced cell-cell adhesion and failure to polarize (41, 42). It is reasonable to speculate that such changes in homotypic interactions may lead to impaired tumor formation and progression beyond single cells.

The fact that over-expression of the T567A mutant resulted in the specific inhibition of metastasis, without a notable impact on primary tumor growth was interesting and suggested an important translational opportunity. The limited metastatic potential of T567A expressing cells may explain why some OS patients develop primary tumors and do not progress to metastasis while most patients will progress despite control of the primary tumor and both neoadjuvant and adjuvant chemotherapy. Studies of a cellular mechanism to explain the inhibition of metastatic progression of EzrinT567A-GFP cells revealed a reduced efficiency in the formation of 3D colonies in soft agar, on collagen I gels or in Matrigel (based on colony size and or number). It is interesting to hypothesize that the ability to overcome the stress of growth on specific substrates or in contact deprived environments is similar to the stress experienced by single metastatic cells arriving in a foreign metastatic environment. Such a hypothesis would link these EzrinT567A-GFP *in vitro* findings to mechanistic studies suggesting the role of EzrinT567A-GFP in early metastatic survival in the lung (*ex vivo* PuMA assay) and finally *in vivo* studies of spontaneous and experimental metastasis. In our studies of metastatic progression in solid tumors, we have been increasingly drawn to the fact that metastatic cells that arrive at distant secondary sites are under considerable cellular stress. We hypothesize that this stress results from the fact that these cells are required to engage a foreign microenvironment and develop paracrine and endocrine signaling cascades often distinct from those needed for growth in the tumor's originating microenvironment or in the primary tumor. In short, the survival of cells at secondary sites is a critical determinant of metastasis (43). Using both murine and human OS cell lines in which we dysregulated Ezrin (expression of EzrinT567A), we found a consistent increase in apoptosis shortly after the arrival of single cells in the lung. These data collectively suggest that transitions between Ezrin conformational forms is necessary to protect cells against stresses faced early after cells arrive at a secondary site.

To address this hypothesis and generate additional hypotheses that could explain how EzrinT567A-GFP expression inhibited metastasis, microarray subtractions between cells expressing EzrinT567A-GFP and wild-type Ezrin were conducted. We were most struck by the consistency of the functions of genes that were upregulated following over-expression of EzrinT567A-GFP. These functions were almost exclusively linked to cellular metabolism or cellular energy. Most notably, these functions suggested a shift in the metabolism of both carbohydrates and amino acids. Considered to be a hallmark of the cancer phenotype, the field of cellular metabolism and cancer has received considerable recent attention (44, 45). At its most basic level, cancer cells appear to be able to manage the production of energy from a number of sources under both aerobic and anaerobic conditions, more effectively than normal cells. Differences in metabolic competency of non-metastatic and metastatic cells have however not been addressed. Using direct measurement of cellular respiration and metabolism we found the over-expression of Ezrin-T567A in cells resulted in reduced cellular respiration (based on lactate production) and reduced oxygen consumption (Fig. 5C & Fig. S3), as well as reduced cellular ATP and ATP dependent oxygen consumption (Fig. S3) compared to wild type cells. The connection between Ezrin dysregulation and altered cell metabolism may not be surprising based on the fact that glycolytic enzymes are known to be associated with the Actin cytoskeleton and these reactions contribute to subcellular functions of cells including signaling reactions between the cell membrane and nucleus (46, 47). Based on these data we hypothesize that metastatic cells with an efficiently regulated Actin cytoskeleton may have a greater fluency and flexibility in managing energetic needs during times of stress than non-metastatic cells and further that the dysregulation of Ezrin leads to an urgent, but failed attempt by cells to correct this metabolic defect. In an attempt

to manage this failing energetic state, cells with mutated Ezrin are forced to enter a less efficient form of metabolism. We hypothesize that this pathway shift and rescue attempt was sufficient to maintain cell viability and many aspects of the cancer phenotype (i.e. invasion, migration, and primary tumor growth); however, the shift was insufficient to meet the energy/metabolic needs of the metastatic cancer cell, especially during the critical stresses that occur early after cellular arrival at distant secondary sites. Indeed, these findings support the extension of our hypothesis that metastatic success may be linked to an ability of cells to efficiently provide and use energy. Recent data from our group suggests that therapeutic strategies that impair the generation and use of cellular energy (e.g. through Metformin treatment) may be uniquely active against the metastatic phenotype of OS (personal communication, manuscript under review).

That both the open and closed conformations of Ezrin are needed for tumor progression and metastasis is consistent with our understanding of the dynamic and complex sequence of events that lead from primary tumor development through the steps of metastatic progression. In regards to metastasis it appears that the transitions between these conformational forms are needed early after metastatic cells arrive in the lung. The biological mechanism that underpins this observation is that transitions between Ezrin conformations is needed to protect cells against apoptotic death at these critical points during metastatic progression. Based on gene expression data and functional validation *in vitro*, we have found an association between the inhibition of metastasis following dysregulation of Ezrin function with alterations in cellular respiration and energy metabolism. Ongoing studies will determine how dysregulation of cellular metabolism is linked to the steps of metastasis and how these data can be translated into rational therapeutic approaches for metastasis.

Supplementary Material

Refer to Web version on PubMed Central for supplementary material.

Acknowledgments

We thank the following for their contributions to the manuscript, Barbara Taylor and Subhadra Banerjee, Nicole Lum, Kunio Nagashima, Kevin Bittman, Deborah Hurtado and James Morrow. Dr. Hue Luu for providing the MG63 and MG63.2 human osteosarcoma cell lines. This research was supported by the NIH Intramural Research Program and NIH grant RO1 CA-22762.

Reference

1. Khanna C, Wan X, Bose S, Cassaday R, Olomu O, Mendoza A, et al. The membrane-cytoskeleton linker ezrin is necessary for osteosarcoma metastasis. Nat Med. 2004; 10:182–186. [PubMed: 14704791]
2. Yu Y, Khan J, Khanna C, Helman L, Meltzer PS, Merlino G. Expression profiling identifies the cytoskeletal organizer ezrin and the developmental homeoprotein Six-1 as key metastatic regulators. Nat Med. 2004; 10:175–181. [PubMed: 14704789]
3. Li Q, Wu M, Wang H, Xu G, Zhu T, Zhang Y, et al. Ezrin silencing by small hairpin RNA reverses metastatic behaviors of human breast cancer cells. Cancer Lett. 2008; 261:55–63. [PubMed: 18155831]
4. Madan R, Brandwein-Gensler M, Schlecht NF, Elias K, Gorbovitsky E, Belbin TJ, et al. Differential tissue and subcellular expressionof ERM proteins in normal and malignant tissues: cytoplasmic ezrin expression has prognostic signficance for head and neck squamous cell carcinoma. Head Neck. 2006; 28:1018–1027. [PubMed: 16783828]

5. Makitie T, Carpen O, Vaheri A, Kivela T. Ezrin as a prognostic indicator and its relationship to tumor characteristics in uveal malignant melanoma. Invest Ophthalmol Vis Sci. 2001; 42:2442–2449. [PubMed: 11581181]
6. Tsukita S, Oishi K, Sato N, Sagara J, Kawai A. ERM family members as molecular linkers between the cell surface glycoprotein CD44 and actin-based cytoskeletons. J Cell Biol. 1994; 126:391–401. [PubMed: 7518464]
7. Reczek D, Berryman M, Bretscher A. Identification of EBP50: A PDZ-containing phosphoprotein that associates with members of the ezrin-radixin-moesin family. J Cell Biol. 1997; 139:169–179. [PubMed: 9314537]
8. Fehon RG, McClatchey AI, Bretscher A. Organizing the cell cortex: the role of ERM proteins. Nat Rev Mol Cell Biol. 11:276–287. [PubMed: 20308985]
9. Nijhara R, van Hennik PB, Gignac ML, Kruhlak MJ, Hordijk PL, Delon J, et al. Rac1 mediates collapse of microvilli on chemokine-activated T lymphocytes. J Immunol. 2004; 173:4985–4993. [PubMed: 15470041]
10. Stanasila L, Abuin L, Diviani D, Cotecchia S. Ezrin directly interacts with the alpha1b–adrenergic receptor and plays a role in receptor recycling. J Biol Chem. 2006; 281:4354–4363. [PubMed: 16352594]
11. Fievet BT, Gautreau A, Roy C, Del Maestro L, Mangeat P, Louvard D, et al. Phosphoinositide binding and phosphorylation act sequentially in the activation mechanism of ezrin. J Cell Biol. 2004; 164:653–659. [PubMed: 14993232]
12. Hamada K, Shimizu T, Matsui T, Tsukita S, Hakoshima T. Structural basis of the membrane-targeting and unmasking mechanisms of the radixin FERM domain. Embo J. 2000; 19:4449–4462. [PubMed: 10970839]
13. Ren L, Hong SH, Cassavaugh J, Osborne T, Chou AJ, Kim SY, et al. The actin-cytoskeleton linker protein ezrin is regulated during osteosarcoma metastasis by PKC. Oncogene. 2009; 28:792–802. [PubMed: 19060919]
14. Geller DS, Gorlick R. Osteosarcoma: a review of diagnosis, management, and treatment strategies. Clin Adv Hematol Oncol. 8:705–718. [PubMed: 21317869]
15. Hong SH, Briggs J, Newman R, Hoffman K, Mendoza A, LeRoith D, et al. Murine osteosarcoma primary tumour growth and metastatic progression is maintained after marked suppression of serum insulin-like growth factor I. Int J Cancer. 2009; 124:2042–2049. [PubMed: 19132750]
16. Khanna C, Khan J, Nguyen P, Prehn J, Caylor J, Yeung C, et al. Metastasis-associated differences in gene expression in a murine model of osteosarcoma. Cancer Res. 2001; 61:3750–3759. [PubMed: 11325848]
17. Su Y, Luo X, He BC, Wang Y, Chen L, Zuo GW, et al. Establishment and characterization of a new highly metastatic human osteosarcoma cell line. Clin Exp Metastasis. 2009; 26:599–610. [PubMed: 19363654]
18. Khanna C, Prehn J, Yeung C, Caylor J, Tsokos M, Helman L. An orthotopic model of murine osteosarcoma with clonally related variants differing in pulmonary metastatic potential. Clin Exp Metastasis. 2000; 18:261–271. [PubMed: 11315100]
19. Werner S, Mendoza A, Hilger RA, Erlacher M, Reichardt W, Lissat A, et al. Preclinical studies of treosulfan demonstrate potent activity in Ewing's sarcoma. Cancer Chemother Pharmacol. 2008; 62:19–31. [PubMed: 17823799]
20. Mendoza A, Hong SH, Osborne T, Khan MA, Campbell K, Briggs J, et al. Modeling metastasis biology and therapy in real time in the mouse lung. J Clin Invest. 2010; 120:2979–2988. [PubMed: 20644255]
21. Available from: http://www.broad.mit.edu/gsea/
22. Available from: http://www.broad.mit.edu/gsea/msigdb/
23. Wu M, Neilson A, Swift AL, Moran R, Tamagnine J, Parslow D, et al. Multiparameter metabolic analysis reveals a close link between attenuated mitochondrial bioenergetic function and enhanced glycolysis dependency in human tumor cells. Am J Physiol Cell Physiol. 2007; 292:C125–C136. [PubMed: 16971499]
24. Wong CW, Lee A, Shientag L, Yu J, Dong Y, Kao G, et al. Apoptosis: an early event in metastatic inefficiency. Cancer Res. 2001; 61:333–338. [PubMed: 11196183]

25. Cameron MD, Schmidt EE, Kerkvliet N, Nadkarni KV, Morris VL, Groom AC, et al. Temporal progression of metastasis in lung: cell survival, dormancy, and location dependence of metastatic inefficiency. Cancer Res. 2000; 60:2541–2546. [PubMed: 10811137]
26. Fidler IJ. Metastasis: guantitative analysis of distribution and fate of tumor embolilabeled with 125 I-5-iodo-2'-deoxyuridine. J Natl Cancer Inst. 1970; 45:773–782. [PubMed: 5513503]
27. Chambers AF, Naumov GN, Vantyghem SA, Tuck AB. Molecular biology of breast cancer metastasis. Clinical implications of experimental studies on metastatic inefficiency. Breast Cancer Res. 2000; 2:400–407. [PubMed: 11250733]
28. Ilmonen S, Vaheri A, Asko-Seljavaara S, Carpen O. Ezrin in primary cutaneous melanoma. Mod Pathol. 2005; 18:503–510. [PubMed: 15475929]
29. Song J, Fadiel A, Edusa V, Chen Z, So J, Sakamoto H, et al. Estradiol-induced ezrin overexpression in ovarian cancer: a new signaling domain for estrogen. Cancer Lett. 2005; 220:57–65. [PubMed: 15737688]
30. Weng WH, Ahlen J, Astrom K, Lui WO, Larsson C. Prognostic impact of immunohistochemical expression of ezrin in highly malignant soft tissue sarcomas. Clin Cancer Res. 2005; 11:6198–6204. [PubMed: 16144921]
31. Gautreau A, Louvard D, Arpin M. Morphogenic effects of ezrin require a phosphorylation-induced transition from oligomers to monomers at the plasma membrane. J Cell Biol. 2000; 150:193–203. [PubMed: 10893267]
32. Weigelt B, Peterse JL, van 't Veer LJ. Breast cancer metastasis: markers and models. Nat Rev Cancer. 2005; 5:591–602. [PubMed: 16056258]
33. Chambers AF, Groom AC, MacDonald IC. Dissemination and growth of cancer cells in metastatic sites. Nat Rev Cancer. 2002; 2:563–572. [PubMed: 12154349]
34. McClatchey AI. Modeling metastasis in the mouse. Oncogene. 1999; 18:5334–5339. [PubMed: 10498886]
35. Khanna C, Jaboin JJ, Drakos E, Tsokos M, Thiele CJ. Biologically relevant orthotopic neuroblastoma xenograft models: primary adrenal tumor growth and spontaneous distant metastasis. In Vivo. 2002; 16:77–85. [PubMed: 12073775]
36. Fais S. Moulding the shape of a metastatic cell. Leuk Res. 34:843–847. [PubMed: 20189645]
37. Pignochino Y, Grignani G, Cavalloni G, Motta M, Tapparo M, Bruno S, et al. Sorafenib blocks tumour growth, angiogenesis and metastatic potential in preclinical models of osteosarcoma through a mechanism potentially involving the inhibition of ERK1/2, MCL-1 and ezrin pathways. Mol Cancer. 2009; 8:118. [PubMed: 20003259]
38. Machesky LM. Lamellipodia and filopodia in metastasis and invasion. FEBS Lett. 2008; 582:2102–2111. [PubMed: 18396168]
39. Di Cristofano C, Leopizzi M, Miraglia A, Sardella B, Moretti V, Ferrara A, et al. Phosphorylated ezrin is located in the nucleus of the osteosarcoma cell. Mod Pathol. 23:1012–1020. [PubMed: 20348881]
40. Oshiro N, Fukata Y, Kaibuchi K. Phosphorylation of moesin by rho-associated kinase (Rho-kinase) plays a crucial role in the formation of microvilli-like structures. J Biol Chem. 1998; 273:34663–34666. [PubMed: 9856983]
41. Pujuguet P, Del Maestro L, Gautreau A, Louvard D, Arpin M. Ezrin regulates E-cadherin-dependent adherens junction assembly through Rac1 activation. Mol Biol Cell. 2003; 14:2181–2191. [PubMed: 12802084]
42. Elliott BE, Qiao H, Louvard D, Arpin M. Co-operative effect of c-Src and ezrin in deregulation of cell-cell contacts and scattering of mammary carcinoma cells. J Cell Biochem. 2004; 92:16–28. [PubMed: 15095400]
43. Tsai YC, Mendoza A, Mariano JM, Zhou M, Kostova Z, Chen B, et al. The ubiquitin ligase gp78 promotes sarcoma metastasis by targeting KAI1 for degradation. Nat Med. 2007; 13:1504–1509. [PubMed: 18037895]
44. Vander Heiden MG, Cantley LC, Thompson CB. Understanding the Warburg effect: the metabolic requirements of cell proliferation. Science. 2009; 324:1029–1033. [PubMed: 19460998]
45. Deberardinis RJ, Sayed N, Ditsworth D, Thompson CB. Brick by brick: metabolism and tumor cell growth. Curr Opin Genet Dev. 2008; 18:54–61. [PubMed: 18387799]

46. Poglazov BF. Actin and coordination of metabolic processes. Biochem Int. 1983; 6:757–765. [PubMed: 6385979]

47. Poglazov BF, Livanova NB. Interaction of actin with the enzymes of carbohydrate metabolism. Adv Enzyme Regul. 1986; 25:297–305. [PubMed: 3544705]

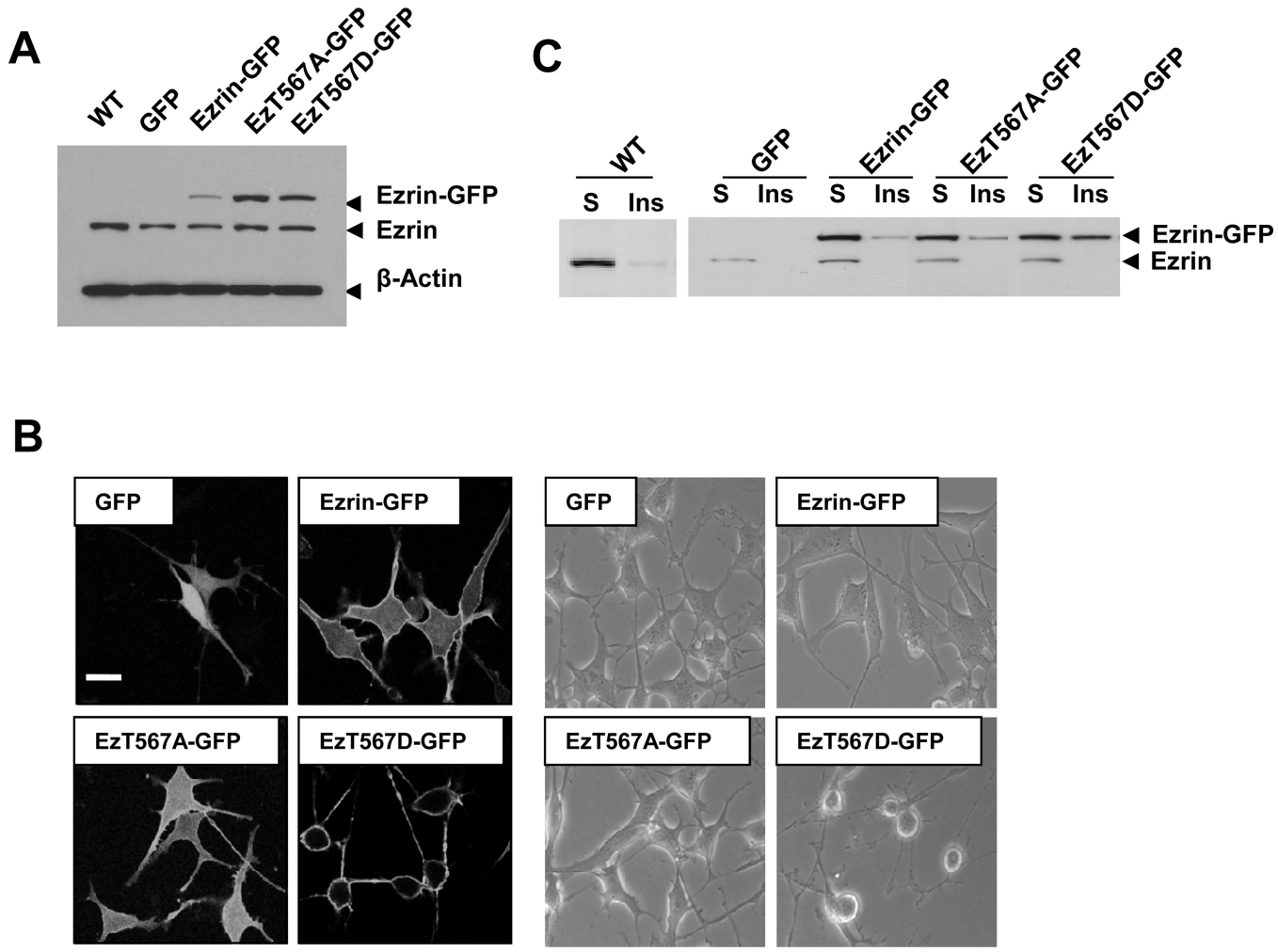

Figure 1. Characterization of EzrinT567 mutant expression in osteosarcoma cells

(A). Western analysis demonstrates the expression of endogenous Ezrin and GFP-tagged Ezrin mutants in K7M2 cells. (B). Localization of GFP and GFP-tagged Ezrin and Ezrin mutants in K7M2 cells was assessed by GFP fluorescence using confocal microscopy. Expression of GFP, Ezrin-GFP, and EzrinT567A-GFP is seen throughout the cytoplasm and cell membrane, whereas EzrinT567D–GFP is largely restricted to the cortical cell membrane. Cell integrity and cellular phenotype is presented by phase contract microscopy (bar=20μm). (C). The subcellular localization of endogenous Ezrin and GFP-tagged Ezrin mutants was confirmed using triton-X 100 fractionation. Ezrin in the triton soluble and insoluble fractions was detected by Western blotting. EzrinT567D–GFP was distributed between the insoluble (Actin rich) and soluble fractions (Actin free) whereas EzrinT567A-GFP was largely expressed in the soluble fractions.

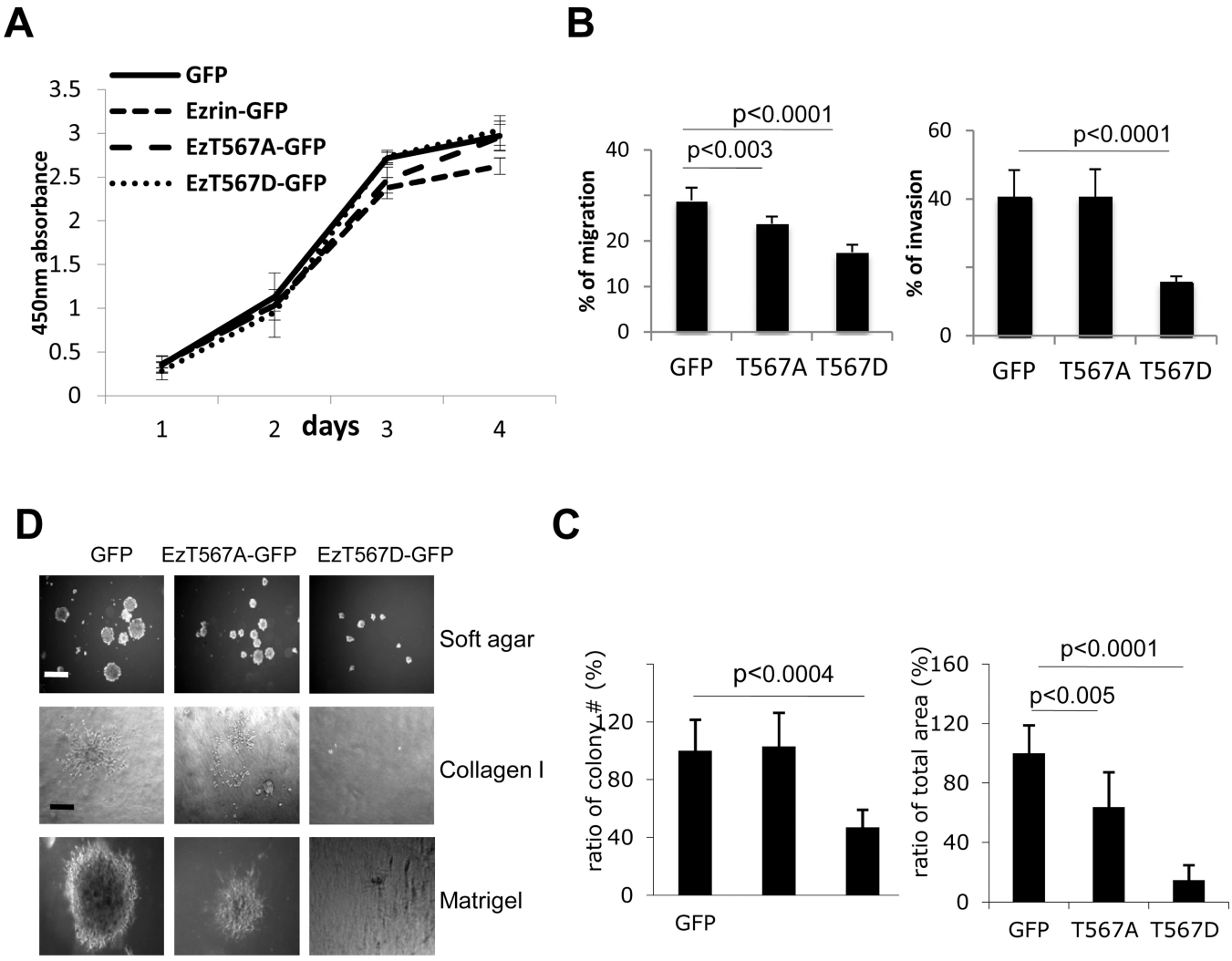

Figure 2. Characterization of the *in vivo* metastatic phenotype of osteosarcoma cells over-expressing EzrinT567 mutants

(A). Cell proliferation analysis of EzrinT567 mutant cell lines. (B). Transwell migration and Matrigel invasion of EzrinT567 mutants. (C). Colony formation in soft agar culture. Cells were suspended in soft agar conditions for 14 days. After 14 days in culture, an image of each well was taken by CCD camera using a Leica MZFLIII microscope. (D) Visualization of colony formation in soft agar (as above) (bar=1mm), on Collagen I or in Matrigel (bar=200μm).

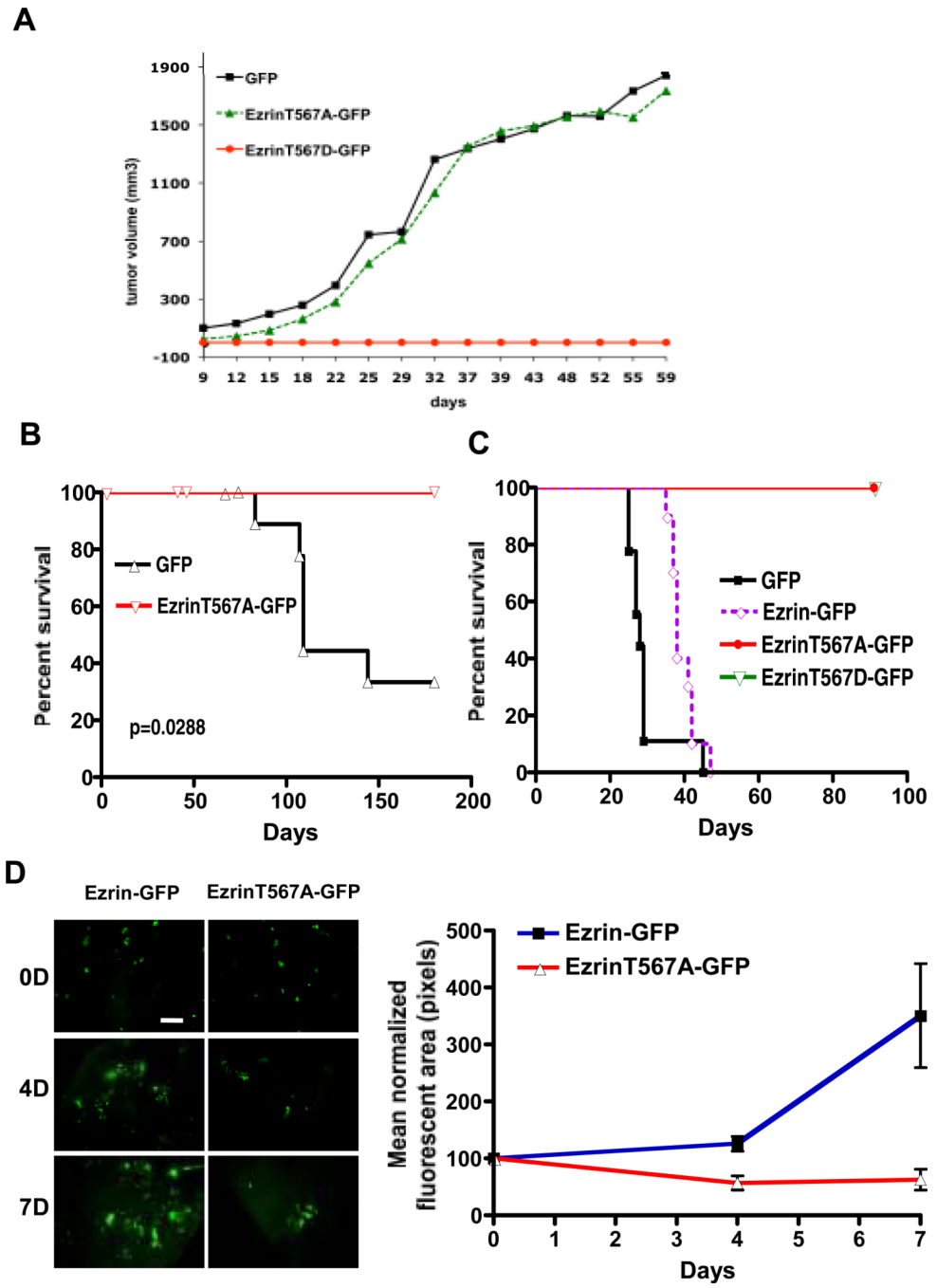

Figure 3. Over-expressing EzrinT567D mutants abrogates primary tumor growth and metastasis while EzrinT567A specifically inhibits metastasis

(A). Orthotopic appendicular primary tumor growth of OS cells expressing GFP alone and EzrinT567-GFP mutants was assessed in mice (n=16–18/group). No growth of primary tumors was seen following injection of EzrinT567D–GFP cells. Expression of GFP and EzrinT567A-GFP fusion proteins within established tumors in mice was confirmed by Western blot (Fig. S2A). (B). Spontaneous metastasis to the lungs, following resection of tumor-bearing limb was assessed. Necropsy assessment to confirmed fulminate metastatic disease in all mice. Results were validated in two replicate experiments of similar size (data not shown). (C). Experimental metastasis assay using OS cells expressing GFP alone, Ezrin-

GFP and EzrinT567-GFP mutants. Cells were delivered by tail vein injection (n=10/group). Mice were then followed for signs of metastasis related morbidity and necropsy confirmed fulminate metastatic disease in all mice. Replicate experiments yielded similar results in distinct cohorts of mice. Similar results were found in human OS cells (MG63.2) (Fig. S2E). (D). Assessment of early metastatic progression using the *ex vivo* PuMA (Pulmonary metastasis assay) revealed impaired function of EzrinT567 mutant expressing cells. The left panel presents fluorescent inverted microscope images from representative *ex vivo* lung culture (PuMA) sections, where green fluorescent events represent tumor cells (bar=200μm). Right panel provides quantification of fluorescent green tumor cells during progression in *ex vivo* lung culture.

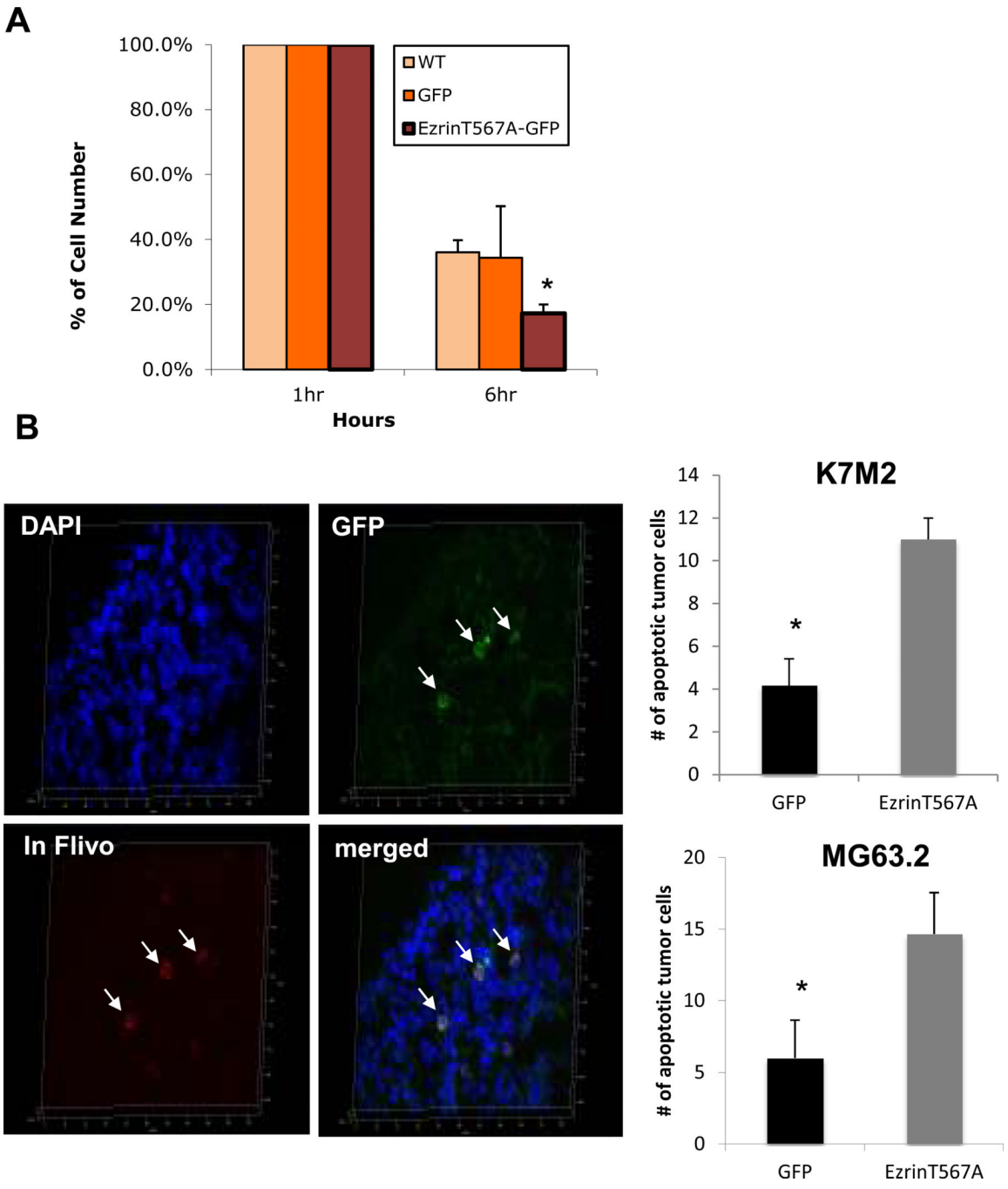

Figure 4. Over-expressing EzrinT567A mutants leads to increased apoptosis of single metastatic cells shortly after their arrival in the lung

(A) Single cell videomicroscopy (SCVM) confirms early loss of EzrinT567-GFP mutant expressing cells following their arrival in the lung. Wild type K7M2 cells and K7M2 cells expressing GFP alone or EzrinT567-GFP mutants assessed by SCVM as previously described (1); * $p<0.05$. (B) Ezrin dysregulation, through EzrinT567A expression, leads to increased apoptosis of single metastatic cells shortly after their arrival in the lung. Fluorescence detection of Caspase activation in single tumor cells *in vivo* was performed with SR-FLIVO using a modification of the single cell videomicroscopy (SCVM) assay (1). Two hours after tail vein injection, murine (K7M2) and human (MG63.2) osteosarcoma

cells expressing EzrinT567A-GFP were found to have significantly greater Caspase activation (apoptosis) than cells expressing GFP alone. * $p<0.05$. The colocalization of red fluorescent SR-FLIVO staining within GFP-expressing tumor cells was confirmed in 15 μm frozen sections by confocal microscopy.

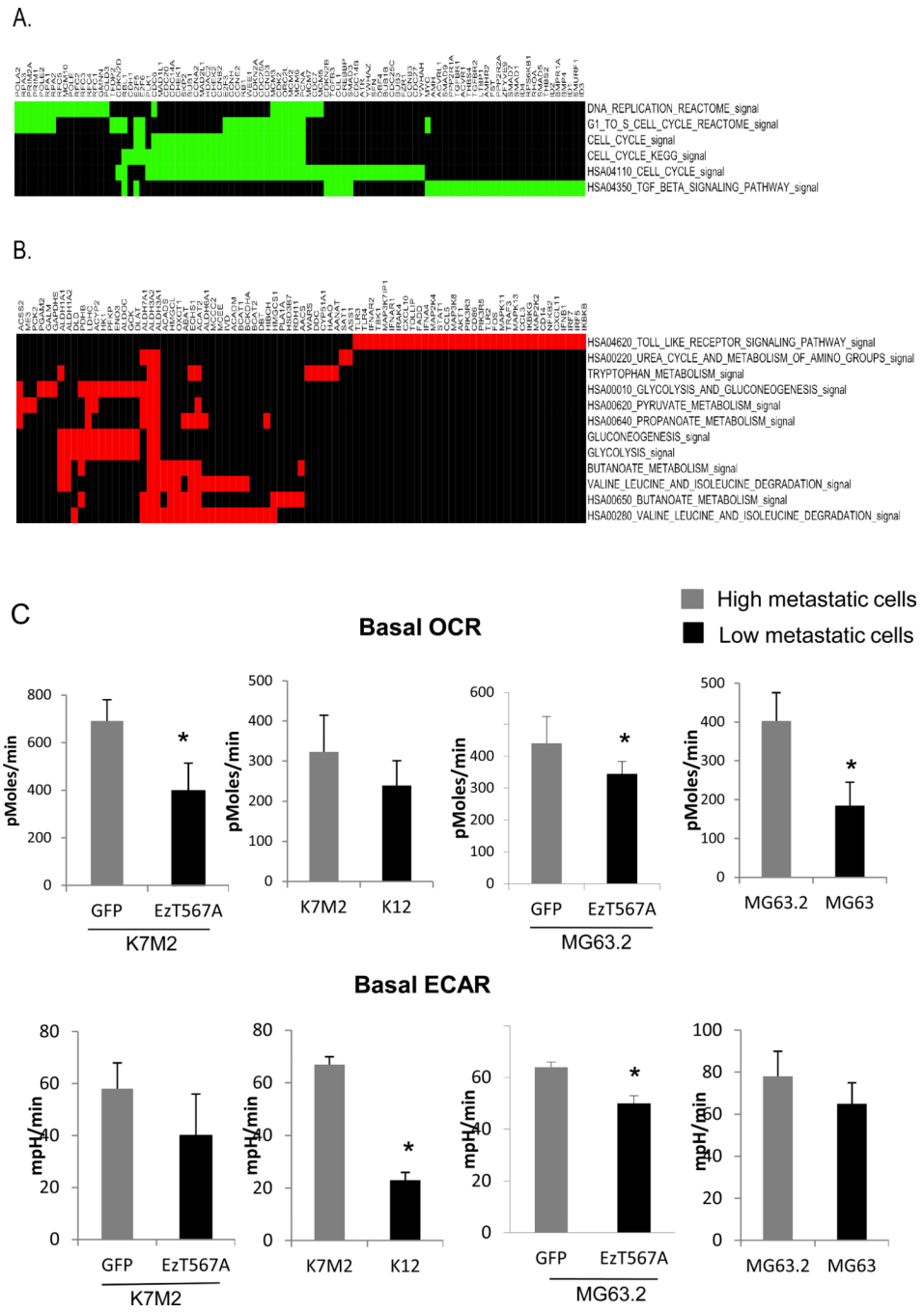

Figure 5. Gene expression studies with functional validation suggest an association between Ezrin-dysregulation and cellular respiration and metabolism

Leading edge subsets from the gene sets significantly down- and up-regulated in T567A–GFP mutants (compared to GFP control) are clustered and plotted in color-maps. (A). Leading edge subsets from the down-regulated gene sets are indicated in green. (B). Leading edge subsets from the up-regulated gene sets are indicated in red. (C). The basal level oxygen consumption rate (OCR) and extracellular acidification rate (ECAR) of cells expressing GFP and EzrinT567A-GFP along with other 2 pairs of high/low metastatic OS cell lines (MG63.2/MG63 and K7M2/K12) were measured with the XF24 Extracellular Flux Analyzer (Seahorse Bioscience). These experiments were repeated for 3 times.

Table 1

Summary of *in vitro* and *in vivo* phenotype of osteosarcoma cells over-expressing Ezrin mutants at T567

	***In vitro* doubling time**[1]	**Migration**[2]	**Invasion**[3]	**Primary tumor growth**[4]	**Spontaneous metastases**[5]	**Experimental metastases**[6]
GFP	20 hours	28.9%	40.6%	68.75% (11/16)	55% (6/11)	100% (10/10)
EzrinT567A–GFP	20 hours	23.8%	40.5%	61.11% (11/18)	0/11 (0%)	0% (0/20)
EzrinT567D–GFP	17 hours	17.6%	15.5%	0% (0/18)	N/A	0% (0/20)

[1] Interpolation from data in figure 2A

[2] Percent of cells undergoing transwell migration figure 2B

[3] Percent of cells undergoing transwell invasion figure 2B

[4] Percent of mice developing orthotopic primary tumors figure 3A

[5] Percent of mice developing spontaneous metastasis from orthotopic primary tumors figure 3B

[6] Percent of mice developing experimental metastasis following tail vein injection of cells, figure 3C

Table 2

Summary of gene set enrichment analysis (EzrinT567A mutants vs. empty vector control)

Gene set name	Number of overlapped genes	Number of genes in the leading edge	Sources	p-value	FDR
Down-regulated in EzrinT567A mutants					
DNA_REPLICATION_REACTOME	39	26	GenMapp	< 0.001	0.000
HSA04350_TGF_BETA_SIGNALING_PATHWAY	82	34	KEGG	< 0.001	0.004
G1_TO_S_CELL_CYCLE_REACTOME	66	27	GenMapp	< 0.001	0.028
HSA04110_CELL_CYCLE	107	49	KEGG	< 0.001	0.046
CELL_CYCLE	72	28	GO	< 0.001	0.044
CELL_CYCLE_KEGG	80	31	KEGG	< 0.001	0.054
Up-regulated in EzrinT567A mutants					
HSA00280_VALINE_LEUCINE_AND_ISOLEUCINE_DEGRADATION	41	21	KEGG	< 0.001	0.012
HSA00640_PROPANOATE_METABOLISM	32	10	KEGG	< 0.001	0.015
HSA00650_BUTANOATE_METABOLISM	42	14	KEGG	< 0.001	0.013
HSA04620_TOLL_LIKE_RECEPTOR_SIGNALING_PATHWAY	92	34	KEGG	< 0.001	0.029
GLUCONEOGENESIS	45	14	GenMapp	< 0.001	0.028
BUTANOATE_METABOLISM	27	12	GenMapp	0.002	0.013
HSA00010_GLYCOLYSIS_AND_GLUCONEOGENESIS	54	16	KEGG	0.002	0.011
HSA00220_UREA_CYCLE_AND_METABOLISM_OF_AMINO_GROUPS	28	5	KEGG	0.002	0.021
HSA00620_PYRUVATE_METABOLISM	38	9	KEGG	0.003	0.061
GLYCOLYSIS	45	14	GenMapp	0.004	0.029
VALINE_LEUCINE_AND_ISOLEUCINE_DEGRADATION	35	16	GenMapp	0.005	0.035
TRYPTOPHAN_METABOLISM	37	10	GenMapp	0.009	0.068